COMPENSATION OF GEOMETRIC AND ELASTIC DEFLECTION ERRORS IN LARGE MANIPULATORS BASED ON EXPERIMENTAL MEASUREMENTS: APPLICATION TO A HIGH ACCURACY MEDICAL MANIPULATOR

P. DROUET [1], S. DUBOWSKY [2], C. MAVROIDIS[3]
[1] *Laboratoire de Mécanique des Solides, Université de Poitiers*
Bât. SP2MI, 86960 Futuroscope, FRANCE, Tél 05.49.49.65.00,

[2] *Massachusetts Institute of Technology,*
Department of Mechanical Engineering
Cambridge, MA 02139, USA, Tel 617-253-2144, Fax 617-258-7881
e-mail: dubowsky@mit.edu

[3] *Department of Mechanical and Aerospace Engineering,*
Rutgers University,
98 Brett Road, Piscataway, NJ 08854, USA, Tel 732-445-0732

Abstract. A model is developed to compensate for end-effector manipulator errors. The objective is to achieve very high accuracy. The method explicitly decomposes measured end-point error data into generalized geometric and elastic errors. It is computationally simple and requires only identification of parameters which are functions of only one variable. It is shown that the measured data requirements are relatively low. The method is applied to a high accuracy 6 DOF medical robot that positions patients for cancer therapy. Experimental results demonstrate the high effectiveness of the compensation method.

1. Introduction

A key element of a new cancer research and treatment facility, being constructed at the Massachusetts General Hospital (MGH) is a robotic patient positioner system (PPS), (see Flanz, et al., 1995; NPTC, 1997). The PPS has to very accurately position patients under a proton beam. The error must be less than ± 0.5 mm over about 5 m. Other medical requirements of the PPS mandate a large workspace of about 3 m, a cantilevered design and a large payload (patient with health care equipment: weight variation from 20 KG to 200 KG). All of these result in an inaccurate system. The errors are due to small geometric errors and elastic deformations of the system's components. Studies showed that the inherent physical errors of the system, particularly those due to elastic effects, are at least 10 times the requirement (Mavroidis, et al.,

1997). In this case, the end-point of the positioner is the tumor of the patient. For medical reasons, no on-line feedback of the end-point is possible. This study was undertaken to solve this problem.

In many industrial applications, considerable research has been performed to improve the accuracy of manipulators without end-effector close-loop control by using model-based calibration methods. Calibration procedures may be separated into three steps: modeling, measurement and identification (Roth, et al., 1987). Working on each of these steps leads to manipulator accuracy improvement. A lot of research has been performed, especially in error model development where models are based on screw theory, homogeneous matrices, Denavit and Hartenberg coordinates, and Jacobian matrices (Hayati, et al., 1988; Mirman and Gupta, 1991). Some models have considered the effects of manipulator kinematic errors (Broderick and Cirpa, 1988; Everett and Lin, 1988; Hollerbach and Wampler, 1996). Others have also added experimentally observed effects, such as backlash and joint compliance (Whitney, et al., 1986). Complete and parametrically continuous (CPC) models are also used (Zhuang, et al., 1993). Some other researchers, while using classical models, focus their work more on the measurement step improvement: using new sensing techniques and equipment, such as mobile camera systems (Zhuang, et al., 1994); laser tracking systems (Vincze, M., et al., 1994; Everett and Lin, 1993); or optimizing the measurement configurations (Borm and Menq, 1991; Zhuang, et al., 1996). Some also improve manipulator performance through local calibration (Everett and Lei, 1995). Finally, identification procedure is also improved in some cases (Zhuang and Roth, 1993). To the best of our knowledge, compensation methods explicitly accommodating for elastic deformation errors under large payload variations have not been developed. Explicitly considering these errors offers the potential for improved accuracy and reduces the amount of data required for implementation.

Here, a serial link manipulator end-effector error model is developed to compensate for geometric and elastic errors. The geometric and elastic errors are explicitly expressed in the model. They are functions of the joint variables and loads applied. The joints can either be revolute or prismatic. The model combines precision and simplicity since errors are described by parameters that are functions of only one variable. Then, the parameter identification process is developed. The parameters are identified from off-line experimental data and are then used to predict the system errors. In practice, these predictions are used to correct for errors during system operation. Finally, the method is experimentally verified on a real system, the PPS. This study shows that it is possible, with relatively low measurement requirements, to fully define the model's parameters and meet the system's accuracy requirements, reducing errors by a factor of 10. The method is now being applied in practice to the PPS at the MGH cancer therapy facility.

2. Geometric and Elastic Error Models

Here, the analytical development leading to the geometric and elastic error model is shown. A classical end-point error kinematic model is developed using generalized errors (Mavroidis, et al., 1997). The errors are considered small to obtain a linearized form of the model. The generalized errors are then decomposed into geometric and elastic errors. These are explicitly determined with parameters that are functions of only one variable.

2.1. KINEMATIC MODEL WITH ERRORS, GENERALIZED ERRORS

Consider an n degree of freedom serial manipulator. The inertial frame F_I is at O_0. The points O_1 to O_n are located at each joint center. The manipulator endpoint is located by a point called O_T. A reference frame F_i is fixed to the i^{th} member at O_{i+1}.

In the following notations, a superscript "i" indicates the ideal position of the end-effector, a superscript "r" indicates the real position. The endpoint frame F_n position and orientation coordinates with respect to the inertial frame form $\mathbf{X}^i_T$, a 6x1 vector: $\mathbf{X}^i_T = [t_x\ t_y\ t_z\ q_x\ q_y\ q_z]^T$. $\mathbf{X}^i_T$ is a nonlinear function of the system geometric parameters and joint variables, respectively **s** and **q**, where the vector **q** is formed by the joint variables q_i (i=1..n) :

$$\mathbf{X}^i_T = \mathbf{f}^i(\mathbf{s},\mathbf{q}) \quad (1)$$

$\mathbf{X}^i_T$ is determined using the well known loop closure equation (Broderick and Cirpa, 1988):

$$\mathbf{A}^i_T = \mathbf{A}_0\ \mathbf{A}_1\ \ldots\ \mathbf{A}_n \quad (2)$$

where $\mathbf{A}_i$ are the classical 4x4 homogeneous matrices that transform frame F_{i-1} to the frame F_i in position and orientation.

Any manipulator will have errors in its geometry, such as link length errors, misalignment of joint axis, etc. So, Equation (1) will not precisely represent the system's kinematics. The errors in the geometry of a manipulator result in the frames defined at the manipulator joints being slightly displaced from their ideal locations. The displacement between the real and the ideal location is represented by a 4x4 homogeneous matrix $\mathbf{E}_i$ (Mavroidis, et al., 1997; Mavroidis, et al., 1997b). The translation part of the matrix $\mathbf{E}_i$ is composed of the 3 displacement coordinates of the F_i^r and F_i^i $\varepsilon_{1,i}$ $\varepsilon_{2,i}$ and $\varepsilon_{3,i}$, the rotation part is the three angles between these frames, $\varepsilon_{4,i}$, $\varepsilon_{5,i}$ and $\varepsilon_{6,i}$. The six parameters, $\varepsilon_{1,i}$ to $\varepsilon_{6,i}$, represent the effect of all the local errors (machining, mounting elastic deformations, ...) in the frame F_i at the end of the link i. These can be defined on a link-by-link basis. The components of E_i are called "generalized error" parameters. For an n degrees of freedom manipulator, there are 6x(n+1) generalized error parameters : $\varepsilon = [\varepsilon_{1,0},\varepsilon_{2,0},\ldots,\varepsilon_{6,0},..,\varepsilon_{1,n},\varepsilon_{2,n},\ldots,\varepsilon_{6,n}]$.
The manipulator loop closure equation becomes:

$$\mathbf{A}^r_T = \mathbf{A}^i_T\mathbf{E}_T = \mathbf{A}_0\ \mathbf{E}_0\ \mathbf{A}_1\ \mathbf{E}_1\ \ldots\ \mathbf{A}_n\ \mathbf{E}_n \quad (3)$$

As with Equation (2), the end-effector coordinates vector $\mathbf{X}^r_T$ can be determined as a function of **s, q**, and ε from Equation (3):

$$\mathbf{X}_T{}^r = \mathbf{f}^r(\mathbf{s},\ \mathbf{q},\ \varepsilon) \quad (4)$$

2.2. A FIRST ORDER APPROXIMATION ON GENERALIZED ERRORS

A linear form of Equation (3) is obtained by assuming that errors in the system are small compared to the size of the manipulator.

The matrix $\mathbf{E}_i$ is then separated in its error part and nonerror part: $\mathbf{E}_i = \mathbf{E}_{ri} + \mathbf{I}$, where **I** is the identity matrix. Using Equation (3) and eliminating second order and higher terms yields the following form of the linearized loop closure equation:

$$\mathbf{A}_0\mathbf{E}_{r0}\mathbf{A}_1\mathbf{A}_2\ldots\mathbf{A}_n+\mathbf{A}_0\ldots\mathbf{A}_i\mathbf{E}_{ri}\mathbf{A}_{i+1}\ldots\mathbf{A}_n+\ldots+\mathbf{A}_0\mathbf{A}_1\ldots\mathbf{A}_n\mathbf{E}_{rn}=\mathbf{A}^r_T-\mathbf{A}^i_T=\mathbf{A}^i_T\mathbf{E}_{rT} \quad (5)$$

For a nonredundant manipulator in a nonsingular configuration, Equation (5) can be multiplied by the inverse of $\mathbf{A}^{i}_{T}$ so that an expression for $\mathbf{E}_{rT}$ is obtained. Matrix $\mathbf{E}_{rT}$ form is similar to matrix $\mathbf{E}_i$ with zeros on the diagonal. Thus the six matrix $\mathbf{E}_{rT}$ elements can be readily identified. Each is a linear function of the generalized errors. The six coordinates of the end-effector error vector $\Delta\mathbf{X}$ can be now obtained from Equation (5) using the linearized form of $\mathbf{E}_{rT}$:

$$\Delta\mathbf{X} = \mathbf{g}(\mathbf{q}, \varepsilon, \mathbf{s}) \tag{6}$$

The matrix form of Equation (6) is given by a generalized errors jacobian:

$$\Delta\mathbf{X} = \mathbf{J}(\mathbf{q}, \mathbf{s})\,\varepsilon \tag{7}$$

where $\mathbf{J}=\partial\mathbf{f}^{r}/\partial\varepsilon$ is a 6 by (6n+6) matrix which can be obtained in explicit algebraic form using symbolic manipulation software such as Maple.

The symbol **s** is dropped from the notation to simplify the expressions.

2.3. GEOMETRIC AND ELASTIC ERRORS, COMPLIANCE PARAMETERS

In this section, it is shown that ε can be formulated so that its components are functions of only one variable. The formulation makes the identification process much easier.

The generalized errors are separated into geometric errors and elastic errors:

$$\varepsilon(\mathbf{q},\mathbf{W}) = \varepsilon_g(\mathbf{q}) + \varepsilon_e(\mathbf{q},\mathbf{W}) \tag{8}$$

where $\varepsilon_e = [\varepsilon_{e0},\varepsilon_{e1},\ldots,\varepsilon_{en}]$ is the elastic error vector, $\varepsilon_g=[\varepsilon_{g0},\varepsilon_{g1},\ldots,\varepsilon_{gn}]$ is the geometric error vector. ε_{gi} and ε_{ei} are 6x1 vectors. Note that while the elastic errors are functions of $\mathbf{q}$ and $\mathbf{W}$, the geometric errors are functions only of $\mathbf{q}$. Equation (7) becomes:

$$\Delta\mathbf{X} = \mathbf{J}(\mathbf{q})\,\varepsilon_g(\mathbf{q}) + \mathbf{J}(\mathbf{q})\,\varepsilon_e(\mathbf{q},\mathbf{W}) = \Delta\mathbf{X_g} + \Delta\mathbf{x_e} \tag{9}$$

where $\Delta\mathbf{X_e}$ is the end-effector error due to elastic deformations only and $\Delta\mathbf{X_g}$ the end-effector error due to geometric errors only.

Equation (9) can be simplified by first noting that, for a manipulator with an open tree configuration, such as a serial manipulator, each joint motion is independent of the others. Therefore the geometric errors ε_{gi} are functions of only the joint variable q_i.

Also, assuming that quasi-static conditions prevail, the wrench at each link can be obtained by simple static analysis. Further, for a quasi-static serial manipulator, the wrench applied to the end of link i at O_{i+1} with respect to the frame F_i, $\mathbf{W}_{i+1,i}$, is only a function of the joint variables following q_i, that is to say q_{i+1}, q_{i+2}, …, q_n, and of the loads applied on links i+1, ..., link n, such as the load applied at the end-effector.

Finally, assuming that the elastic deformations of the i^{th} link are linear with $\mathbf{W}$ leads to:

$$\varepsilon_{ei} = \mathbf{C}_i(q_i)\,\mathbf{W}_{i+1,i}([q_{i+1},\ldots q_n],\mathbf{W}) \tag{10}$$

where $\mathbf{C}_i$ is a 6x6 compliance matrix for the link i. The matrix $\mathbf{C}_i$ is a function of the geometry of the link. For a rotary joint, the geometry of a link does not change, so that $\mathbf{C}_i$ is constant. For a prismatic joint, the length of link i changes with q_i, so the elements of $\mathbf{C}_i$, c_{ijk}, called compliance parameters, are only functions of q_i.

Since ε_{ei} is linear with respect to the compliance parameters and $\Delta\mathbf{X}_e$ is linear with ε_{ei}, $\Delta\mathbf{X}_e$ is linear with the compliance parameters too. (9) and (10) becomes:

$$\Delta\mathbf{X}_e = \mathbf{J}\,[\ldots,\mathbf{C}_i,\ldots]\,[\ldots,\mathbf{W}_{i+1,i},\ldots]^{T} = \mathbf{M_e}(\mathbf{q},\mathbf{W})\,\mathbf{c} \tag{11}$$

where $\mathbf{c}$ is a vector formed from the 36 elements of $\mathbf{C_i}$ (i=0,...,6), $\mathbf{c}=[\mathbf{c_0},\mathbf{c_1}(q_1),\ldots,\mathbf{c_n}(q_n)]$, and $\mathbf{M_e}$ is the end-effector errors jacobian with respect to the compliance parameters: $\mathbf{M_e}=\partial\Delta\mathbf{X_e}/\partial\mathbf{c}$. The matrix $\mathbf{M_e}$ can be obtained in explicit symbolic form.

Finally, Equation (9) and Equation (11) combined give the geometric and elastic error model of the end-effector errors:

$$\Delta\mathbf{X} = \Delta\mathbf{X_g} + \Delta\mathbf{X_e} = \mathbf{J}(\mathbf{q})\,\varepsilon_g + \mathbf{M_e}(\mathbf{q},\mathbf{W})\,\mathbf{c} \qquad (12)$$

Since $\varepsilon_g=[\varepsilon_{g0},\varepsilon_{g1}(q_1),\ldots,\varepsilon_{gn}(q_n)]$ and $\mathbf{c}=[\mathbf{c_0},\mathbf{c_1}(q_1),\ldots,\mathbf{c_n}(q_n)]$. The end-effector errors can be expressed with parameters that are only functions of one variable.

With this model, for the prediction of the end-effector errors, $\mathbf{M_e}$ and $\mathbf{J}$ being explicitly determined, ε_g and $\mathbf{c}$ vectors must be identified from experimental data. The vector ε_g is a 6xn vector and $\mathbf{c}$ is a 36x(n+1) vector. Note that the number of vector $\mathbf{c}$ terms will be significantly reduced in most of the cases. Some simple knowledge of the system's physics such as symmetries in links geometry can be used to simplify the form of the compliance matrices.

3. Parameter Identification Process

The identification process is composed of two steps: the first is the compliance parameter identification, the second is the geometric error parameter identification.

3.1 COMPLIANCE PARAMETER IDENTIFICATION*:*

Equation (12) shows that only $\mathbf{M_e}$ depends on $\mathbf{W}$. Therefore, at a given configuration, the difference between Equation (12) with some weight $\mathbf{W_i}$ and Equation (12) with some other weight $\mathbf{W_j}$ eliminates the geometric errors and gives:

$$\Delta\mathbf{X}(\mathbf{q},\mathbf{W_j}) - \Delta\mathbf{X}(\mathbf{q},\mathbf{W_i}) = [\mathbf{M_e}(\mathbf{q},\mathbf{W_j}) - \mathbf{M_e}(\mathbf{q},\mathbf{W_i})]\,\mathbf{c}(\mathbf{q}) \qquad (13)$$

The left hand side of Equation (13) is the difference between measured errors at two weights and for one configuration. Calculating $\mathbf{M_e}(\mathbf{q},\mathbf{W_i})$ and $\mathbf{M_e}(\mathbf{q},\mathbf{W_j})$ permits Equation (13) to be solved for $\mathbf{c}$ at $\mathbf{q}$. The number of weight pairs required depend on the size of $\mathbf{c}$. When rotary joints are involved, $\mathbf{c}$ is independent of configuration. So any single rotary joint configuration may be used to solve Equation (11). For prismatic joints, the compliance parameters for the i^{th} link are functions only of q_i. Therefore, measuring each prismatic joint independently from the other joints is sufficient to identify the compliance parameters.

3.2 GEOMETRIC ERROR PARAMETER IDENTIFICATION

With $\mathbf{c}$ known and $\mathbf{M_e}$ determined, $\Delta\mathbf{X_e}$ is known. The error vector $\Delta\mathbf{X_g}$ can be determined by taking the difference between end-effector error measured, $\Delta\mathbf{X}$, and the end-effector elastic errors calculated, $\Delta\mathbf{X_e}$:

$$\Delta\mathbf{X_g}(\mathbf{q}) = \Delta\mathbf{X}(\mathbf{q},\mathbf{W}) - \Delta\mathbf{X_e}(\mathbf{q},\mathbf{W}) = \mathbf{J}(\mathbf{q})\,\varepsilon_g(\mathbf{q}) \qquad (14)$$

The matrix $\mathbf{J}$ can be determined at $\mathbf{q}$ from its symbolic expression. The vector ε_g depends on $\mathbf{q}$ and thus can't be identified directly by assembling Equation (14) for various configurations. The vector ε_{gi} depends only on q_i, so, measuring errors while

only joint i moves makes only ε_{gi} vary in Equation (14), the other ε_{gj} ($j \neq i$) keeping their initial value (defined at home configuration, $\mathbf{q}=0$). Thus, ε_{gi} at q_i, are identified by subtracting the end-effector geometric error at home from the error at $\mathbf{q}$. We call this difference $\Delta\mathbf{X_g'}$ which can be written:

$$\Delta\mathbf{X_g'} = \Delta\mathbf{X_g}(\mathbf{q}) - \Delta\mathbf{X_g}(\mathbf{0}) = \mathbf{J}(\mathbf{q})\,\varepsilon_g(\mathbf{q}) - \mathbf{J}(\mathbf{0})\,\varepsilon_g(\mathbf{0}) \tag{15}$$

Equation (15) can be expressed as:

$$\Delta\mathbf{X_g'} = \mathbf{J}(\mathbf{q})\,\Delta\varepsilon_g(\mathbf{q}) + \Delta\mathbf{J}(\mathbf{q})\,\varepsilon_g(\mathbf{0}) \tag{16}$$

where $\Delta\varepsilon_g(\mathbf{q}) = [\varepsilon_g(\mathbf{q}) - \varepsilon_g(\mathbf{0})]$; $\Delta\mathbf{J}(\mathbf{q}) = [\mathbf{J}(\mathbf{q}) - \mathbf{J}(\mathbf{0})]$

Equation (16) is the basic equation used for the geometric error parameter identification. If joint errors are measured independently it is possible to obtain the values of $\varepsilon_g(\mathbf{0})$ and $\Delta\varepsilon_g(\mathbf{q})$ from Equation (16).

4. Application to the Patient Positioner System

4.1. PATIENT POSITIONER SYSTEM DESCRIPTION

The PPS of Northeast Proton Therapy Center (NPTC) at Massachusetts General Hospital is shown in Figure 1. A nozzle delivers a proton beam to the patient. The nozzle is carried by a large rotating gantry. The patient is carried by the end-effector of the PPS manipulator (Flanz, et al. 1996).

The gantry rotation changes the angle of the beam. The point of intersection of the gantry axis of rotation and of the beam is called the "isocenter." The PPS has to place the patient inside the gantry so that the tumor and the isocenter are coincident. The maximum acceptable radial error between the nominal tumor position and the isocenter is 0.5 mm. Larger errors may result in the destruction of healthy tissue. Tests have shown that the PPS cannot achieve this accuracy without error compensation algorithms. The inherent accuracy of the PPS is approximately 5 mm to 8 mm because of its size and its cantilever design.

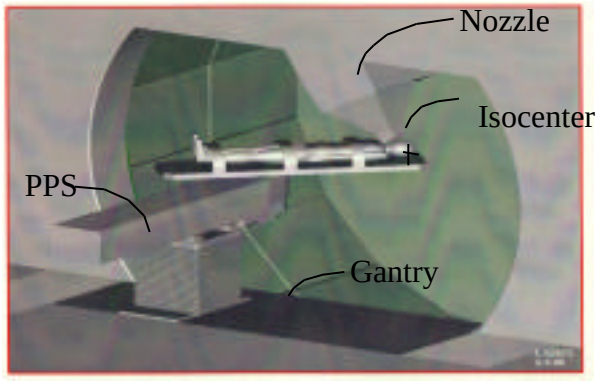

Figure 1: NPTC Patient Positioner System

The PPS is shown in more detail in Figure 2. It is a six DOF manipulator designed by General Atomics, San Diego, CA. The first three joints are prismatic. The maximum travel of these joints is 225 cm for the lateral (X) axis, 56 cm for the vertical

(Y) axis and 147 cm for the longitudinal (Z) axis. The last three joints are revolute joints. The first joint has an axis of rotation parallel to the vertical (Y) axis and can rotate ±90deg. The last two joints are used for small corrections around an axis of rotation parallel to the Z (roll) and X (pitch) axes, and have a maximum rotation angle of ±3deg. The manipulator "end-effector" is a couch which supports the patient in a supine position. The design accommodates supine patients up to 188 cm in height and up to 200 KG in weight in normal operations. The couch treatment volume is defined by a treatment area on the couch of 50 cm x 50 cm and a height of 40 cm.

The reference frames (except F_4 and F_5) are shown in Figure 2. The inertial frame F_I and the frame F_0 are similar and fixed at the base of the system. The frame F_1 moves with the first prismatic joint along the X direction, and is aligned with F_0 at the home position (position where all the joint variables are equal to zero). The frame F_2 moves with the top of the second linear joint in the Y direction. The frame F_3 moves with the end of the arm in the Z direction. F_4 rotates around the vertical axis of the frame 3. F_6 is the reference system defined at the treatment point, such as the tumor in the patient's body. A detail of the treatment area is shown in Figure 4.

The payload (patient, healthcare equipment and couch) wrench are measured by a 6 axis force/torque sensor placed between the couch and the last joint. This sensor gives the patient weight w_p and CG position on the couch (x_p, z_p).

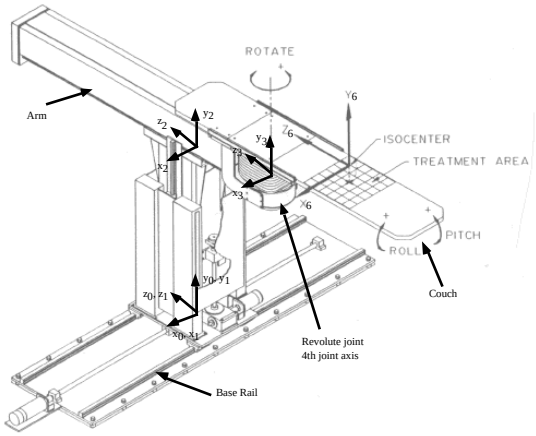

Figure 2: Close view of the PPS, Reference Frames

4.2. ERROR COMPENSATION RESULTS FOR THE PPS

The errors of the PPS are measured using a Leica 3D Laser Tracking System. Three cateye laser targets are mounted on the top of the couch in a triangle configuration around the vertical rotary axis 10 mm above the couch. The center of the triangle $P_1P_2P_3$ is considered as the PPS end-point, O_T. The end-effector frame Y_T is the vector perpendicular to the (P_1 P_2 P_3) plane. X_T axis is the direction of the vector P_2P_3, and Z_T axis is the cross product of X_T and Y_T. The errors are obtained by subtracting the measured frame position and orientation from their ideal values. The accuracy of the PPS position measurements at the 3D measurement points is estimated to be 0.04 mm.

A total of 270 measurements were performed at the Nominal Treatment Point (NTP) located 100 mm above the treatment area center. From these measurements, the repeatability of the PPS system is estimated to be 0.15 mm in 98.6% of the cases.

The measured uncompensated errors in the system are in the 5 to 8 mm range. Hence the assumption that the errors are small compared to the size of the system is satisfied. Furthermore, since the system is stationary during treatment, the quasi-static assumption is also satisfied. The linearity of the elastic deformations with respect to the load has also been verified. The nonlinear effects of **W** were measured to be under 0.041 mm for a payload on the couch varying from 0.0 to 150.0 KG.

Since the PPS is a six degree of freedom manipulator, 36 geometric error parameters have to be identified. The number of compliance parameters is reduced to twelve based on system geometry and loading. Also, since the PPS loading is only due to gravity, and since the range of motion of the pitch and roll axis is very small, the wrench applied to each link has the form: $\mathbf{W} = [\ 0\ F_y\ 0\ M_x\ 0\ M_z\ ]$. The compliance parameters multiplied by zeros in Equation (10) don't influence the elastic errors and hence don't need to be considered by the correction algorithm.

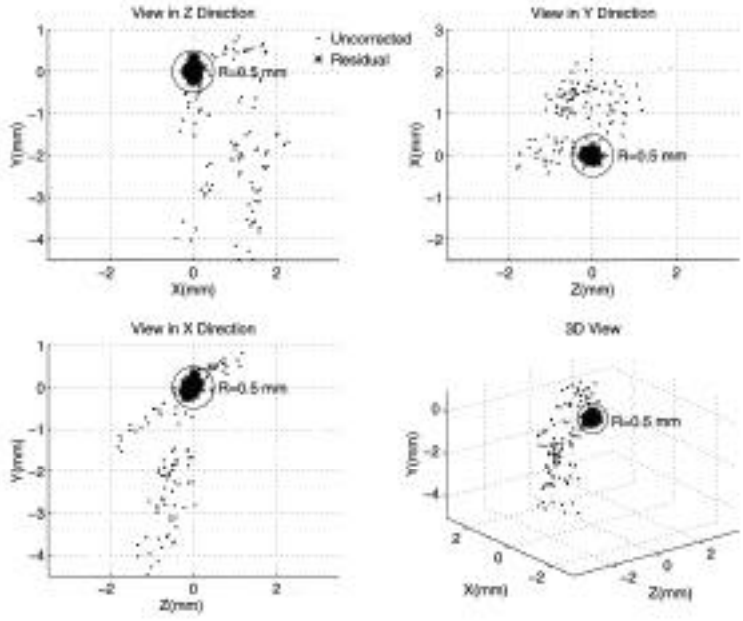

Figure 3: Comparison of NTP uncorrected and residual errors

To determine the error parameters, a series of measurements were made where each joint was moved one at a time with a 50 mm step for joint 1, a 20 mm step for joint 2, a 25 mm step for joint 3, a 5 degree step for joint 4 and half degree steps for joints 5 and 6. This gave a total of 514 measurement configurations. Of these measurements, 191 measurements were performed without any weight on the couch, and 323 had a 70 KG couch load at the nominal treatment point.

In addition to the 512 measurements used for the parameter identification, a set of 110 independent treatment configurations were measured to verify the accuracy of the correction algorithm.

The parameter identification computation, implemented in Matlab, required less than one hour computer time. The accuracy of the end-effector error components is shown in Figure 3. The inherent uncorrected errors of the PPS are shown as dots. The residual errors that are not compensated for by the correction algorithm are shown as

stars. The 0.5 mm specification circle is shown in plain lines. Clearly, the compensation algorithm reduces the errors by approximately a factor of 10, and enables the PPS to meet its specifications.

The distribution of the residual errors shows that 98.6% of the remaining errors at NTP are under 0.4 mm. In this study, it was also shown that the algorithm worked well even if the number of identification points was reduced to only 270.

5. Conclusion

In this paper, a method to compensate for the geometric errors and elastic errors is developed. In the method, a model of the end-point errors of the system is developed in terms of geometric and compliance parameters. These are identified off-line using experimental measurements. The models then are used to correct for errors during system operation. The method is applied to the new high accuracy medical manipulator, the Patient Positioner System. The experimental results show that very good accuracy is obtained enabling this system to meet its design specifications. The method is relatively simple, inexpensive and requires small computational effort. It does not require any measurements during system operation and needs only a relatively low number of measurements for parameter identification.

6. Acknowledgments

Support for this work by the University of Poitiers “Laboratoire de Mécanique des Solides”, the Northeast Proton Therapy Center of Massachusetts General Hospital, NASA and PPS technical information provided by General Atomics, San Diego, CA, are acknowledged and appreciated.

7. References

Borm, J., and Menq, C. (1991) Determination of Optimal Measurement Configurations for Robot Calibration Based on Observability Measure, *The international Journal of Robotics Research*, Vol. 10, No. 1, Febuary 1991.

Broderick, P. and Cirpa, R. (1988) A Method for Determining and Correcting Robot Position and Orientation Errors Due to Manufacturing, *Transactions of the ASME, Journal of Mechanisms, Transmissions and Automation in Design*, 110: 3-10.

Craig, J. (1989) *Introduction to Robotics: Mechanics and Control*, Addison Willey.

Everett, L. and Lei, J. (1995) Improved Manipulator Performance Thrgough Local D-H Calibration , *Journal of Robotics Systems*, 12(7), 505-514.

Everett, L. and Ives, T. (1993) A Sensor Used for Measurements in the Calibration of Production Robots, *IEEE 1993.*

Everett, L. and Lin, C. Y. (1988) Kinematic Calibration of Manipulators with Closed Loop Actuated Joints, *IEEE1988.*

Flanz J., et al., (1995) Overview of the MGH-Northeast Proton Therapy Center plans and progress, *Nuclear Instruments and methods in Physics Research B*, Vol. 99, 830-834.

Flanz, J., (1995) Large medical gantries, Proceeding of the 1995 Particle Accelerator Conference, April, 1995.

Flanz, J., et al. (1996) Design approach for a highly accurate patient positioning system for NPTC, Proceeding of the PTOOG XXV and Hadrontherapy Symposium, Belgium, September, 1996.

Hayati, S., Tso, K., and Roston, G. (1988) Robot geometry calibration, *IEEE 1988.*

Hollerbach, J. and Wampler, C. (1996) The calibration index and taxonomy for robot kinematic calibration methods, *The international Journal of Robotics Research*, Vol. 15, No. 6, December 1996, 573-591.

Mavroidis C., Dubowsky S., Drouet P., Hintersteiner J. and Flanz J. (1997) A systematic error analysis of robotic manipulators: application to a high performance medical robot, Proceedings of the 1997 International Conference in Robotics and Automation, April, 1997

Mavroidis C., Flanz, J., Dubowsky S., Drouet P. and Gotein, M. (1997b) High performance medical robot requirements and accuracy analysis, Submitted to the Journal of Robotics and Computer Integrated Manufacturing.

Mirman, C. and Gupta, K. (1991) Robot parameter identification and compensation using sets of jacobian matrices, *Eighth World Congress on the Theory of Machines and Mechanisms*, Prague, Czechoslovakia, August 26-31, 1991

NPTC, 1997, Webpage of the northeast proton therapy center at the Massachusetts General Hospital, http://www.mgh.harvard.edu/depts/nptc/nptc.htm

Roth, Z., Mooring, B. and Ravani, B. (1987) An overview of robot calibration, *IEEE Journal of Robotics and Automation*, Vol. RA-3, No. 5, October 1987

Vincze, M., Prenninger, J. P., Gander, H. (1994) A laser tracking system to measure position and orientation of robot end effectors under motion, *The International Journal of Robotics Research*, Vol. 13, No.4, 305-314, August 1994

Whitney, D.E., Lozinski, C.A. and Rourke, J.M. (1986) Industrial robot forward calibration method and results, *Journal of Dynamics Systems, Measurement, and Control*, Vol. 108, March 1986

Zhuang, H., Roth, Z. and Wang, K. (1994) Robot calibration by mobile camera systems, *Journal of Robotic Systems*, 11(3), 155-167.

Zhuang, H., Wu, J. and Huang, W. (1996) Optimal planning of robot calibration experiments by genetic algorithms, *Proceedings of the 1996 IEEE International Conference on Robotics and Automation*, Mineapolis, Minnesota, April 1996

Zhuang, H, Wang, L.K., and Roth, Z.S. (1993) Error-model-based robot calibration using a modified cpc model, *Robotics & Computer Integrated Manufacturing*, Vol. 10, No. 4, 287-299.

Zhuang, H. and Roth, Z S. (1993) A linear solution to the kinematic parameter identification of robot manipulator, *IEEE 1993*